Progress In Electromagnetics Research B, Vol. 71, 167–181, 2016

Theoretical Modelling of Kelvin Helmholtz Instability Driven by an Ion Beam in a Negative Ion Plasma

Kavita Rani[1] and Suresh C. Sharma[2, *]

Abstract—An ion beam propagating through a magnetized plasma having positive ions K^+ (Potassium ions), electrons and negative ions SF_6^- (Sulphur hexafluoride ions) drives Kelvin Helmholtz Instability (KHI) via Cerenkov interaction. For two modes, K^+ and SF_6^-, the frequency and the growth rate of the unstable wave increase with the relative density of negative ions. It is observed that the beam has destabilizing effect on the growth rate of KHI in the presence of negative ions. However, at the large concentration of the negative ions beam stabilizes the growth rate of KHI. An increase in mass of negative ions also stabilizes the growth rate of KHI modes. It is also observed that increase in ion beam velocities and densities play a significant role in changing the growth rate of KHI modes. Moreover, the finite geometry effects tend to modify the dispersion properties and growth of KHI modes.

1. INTRODUCTION

The study of Kelvin Helmholtz instability has received great attention in various geophysical and astrophysical situations such as Earth's polar cusps [1], Earth's Magnetosphere [2–5], Comet tails [6] and Ion Loss on Mars [7] etc..

Kelvin Helmholtz instability (KHI) is low frequency perturbation that may arise due to relative motion between the different layers of a conductive, magnetized and incompressible heterogeneous fluid that feeds on the ambient flow energy. The instability may arise in the plasma streaming parallel to the magnetic field whose velocity varies in the direction perpendicular to the magnetic field [8]. The study of the KHI for magnetized compressible fluids showed that the KHI may occur if the relative speed between two adjacent layers exceeds the root mean square Alfven speed between the layers [9]. The essential features of KHI were later on confirmed by experimental observations of Q-machine [10]. The Landau damping has a stabilizing effect on the Kelvin Helmholtz instability [11].

It was observed that the excitation of KHI in a magnetized plasma having positively charged dust grains is easier than negatively charged dust grains due to reduction in the critical shear with increase in the quantity $Z\varepsilon$ (where Z is the charge state and ε is the ratio between dust density and the ion density) for the positive ions [12]. The presence of negative ions has a destabilizing effect on the KHI in a plasma for ion acoustic and electrostatic ion cyclotron (EIC) waves [13]. An et al. [14] have investigated the unstable nature of KHI in a plasma having negative ions and found that the wave amplitude grows as the concentration of negative ions increases. However, relatively large negative ion concentration has stabilizing effect on the K-H instability.The stabilizing effect of negatively charged dust grains on the K-H instability in a magnetized Cesium plasma have also been studied [15].

Moreover, the study of negative ions in the plasma has found to be a source of motivation due to their potential applications in surface plasma technologies [16] such as ion implantation, chemical

Received 23 September 2016, Accepted 17 November 2016, Scheduled 2 December 2016

* Corresponding author: Suresh C. Sharma (suresh321sharma@gmail.com).

[1] Department of Applied Physics, Bhagwan Parshuram Institute of Technology, Sector-17, Rohini, New Delhi 110 089, India. [2] Department of Applied Physics, Delhi Technological University (DTU), Shahbad Daulatpur, Bawana Road, Delhi 110 042, India.

vapour deposition (CVD), etching in ultra-large scale integration (ULSI) fabrications, macro and Nano particles creations [17, 18].

The destabilizing effect of ion beam has been studied by Sharma and Srivastava [19] on the excitation of ion cyclotron (IC) waves in a plasma cylinder with negative ions. Sharma and Gahlot [20] have studied that an ion beam propagating through the magnetized plasma cylinder with negative ions drives electrostatic ion acoustic waves to instability via Cerenkov interaction. The results of their theory showed the increase in phase velocity and unstable mode frequency with negative ions and are in compliance with the experimental observations of Song et al. [21] The dispersion properties of various ion wave modes are modified in the presence of negative ions [22–24]. Various plasma instabilities have been studied in the plasma having negative ions with and without beam. It has been observed earlier in ion beam plasma systems that the beam plays an important role in growth of instabilities [25, 26].

In this paper, we develop a theoretical model on KHI driven by an ion beam in a negative ion plasma as no work on the effect of ion beam on KHI in a magnetized plasma having negative ions has been reported so far. We also study the effects of finite boundaries on the growth of KHI modes as it is observed that finite geometry effects tend to reduce the growth of waves and instabilities [27]. We choose SF_6^- negative ions as SF_6 has a large electron capture cross section for low-energy electrons in Q-machine plasmas [21]. In Section 2, we carry out the instability analysis for two modes (positive ion K^+ and negative ion SF_6^-). The plasma and beam responses are obtained using fluid theory. We obtain the mode frequencies and the growth rate for both the modes using first order perturbation theory. Results and discussions are given in Section 3. Section 4 concludes the results obtained.

2. INSTABILITY ANALYSIS

Consider a fully ionized multi-component collisionless plasma consisting of electrons, positive ions K^+ (Potassium ions) and negative ions SF_6^- (Sulphur hexafluoride ions) immersed in the magnetic field B_s. The magnetic field is the positive z-direction and equilibrium densities of components $j(= e, +, -)$ vary along negative x-direction as $n_{0j} = \overline{n_{0j}} e^{-\lambda x}$, where for different components, $\overline{n_{0j}}(=$ constant) and λ is the e-folding wave vector of the density gradient [15]. Equilibrium densities of electrons, positive ions and negative ions are represented as $n_{0e}(= (1-\varepsilon)n_p), n_{0+} = n_p$ and $n_{0-} = \varepsilon n_p$, where $\varepsilon(= n_{SF_6^-} \Big/ n_{K^+})$ is the relative density of negative ions and n_p is the plasma density. Their charges, masses and temperatures are denoted by $(-e, m_e, T_e), (e, m_+, T_+)$ and $(-e, m_-, T_-)$, respectively. The equilibrium velocity vectors of each components are given by $v_{0j} = (0, v_{0yj}, v_{0zj}(x))$ with $v_{0yj}(=$ constant). An ion beam with velocity $v_{0b} \parallel \hat{z}$, mass m_b, density $n_{0b} \ll n_{0+}$ propagates through plasma along the magnetic field.

Apply quasineutrality on the beam plasma system so that $en_{0e} - en_{0+} - en_{ob} + en_{0-} \approx 0$ as we have taken plasma density $\gg$ beam density.

The motion of all the three plasma species (electrons, positive ions and negative ions) is described by the momentum and continuity equations following the treatment of Sharma & Srivastava [19] (cf. Eqs. (1)–(6)).

Now the equilibrium is perturbed by an electrostatic perturbation to the potential

$$\phi_1 = \phi(r) e^{-i(\omega t - \overrightarrow{k} \cdot \vec{r})}. \tag{1}$$

The first order quantities are assumed to vary as $e^{-i(\omega t - k_y y - k_z z)}$. The response of plasma electrons to the perturbation may be derived from the momentum conservation equation, i.e.,

$$m_e \frac{d\overrightarrow{v_e}}{dt} = -e\overrightarrow{E} - \frac{e}{c}\overrightarrow{v_e} \times \overrightarrow{B_s} - \frac{\nabla(n_e T_e)}{n_e}. \tag{2}$$

We obtain electron, positive ion and negative ions perturbed density from the mass conservation equation as

$$n_{1e} = n_{0e} \frac{e\phi_1}{T_e}. \tag{3}$$

$$n_{1+} = \frac{n_{0+}e\phi_1}{m_+}\frac{\left(\frac{\nabla_\perp^2}{\left(\omega_{c+}^2-\Omega_+^2\right)}+\frac{k_z^2}{\Omega_+^2}+\frac{\lambda k_y\omega_{c+}}{\Omega_+\left(\omega_{c+}^2-\Omega_+^2\right)}-\frac{k_yk_z\omega_{c+}}{\Omega_+^2\left(\omega_{c+}^2-\Omega_+^2\right)}\frac{\partial v_{0z+}}{\partial x}\right)}{\left(1-\frac{\nabla_\perp^2 v_{t+}^2}{\left(\omega_{c+}^2-\Omega_+^2\right)}-\frac{k_z^2v_{t+}^2}{\Omega_+^2}-\frac{\lambda k_yv_{t+}^2\omega_{c+}}{\Omega_+\left(\omega_{c+}^2-\Omega_+^2\right)}+\frac{k_yk_zv_t{}^{+2}\,\omega_{c+}}{\Omega_+^2\left(\omega_{c+}^2-\Omega_+^2\right)}\frac{\partial v_0z+}{\partial x}\right)}. \quad (4)$$

$$\text{and } n_{1-} = \frac{-n_{0-}e\phi_1}{m_-}\frac{\left(\frac{\nabla_\perp^2}{\left(\omega_{c-}^2-\Omega_-^2\right)}+\frac{k_z^2}{\Omega_-^2}-\frac{\lambda k_y\omega_{c}-}{\Omega_-\left(\omega_{c-}^2-\Omega_-^2\right)}+\frac{k_yk_z\omega_{c}-}{\Omega_-^2\left(\omega_{c-}^2-\Omega_-^2\right)}\frac{\partial v_0z-}{\partial x}\right)}{\left(1-\frac{\nabla_\perp^2 v_t{}^{-2}}{\left(\omega_{c-}^2-\Omega_-^2\right)}-\frac{k_z^2v_{t-}^2}{\Omega_-^2}+\frac{\lambda k_yv_{t-}^2\omega_{c-}}{\Omega_-\left(\omega_{c-}^2-\Omega_-^2\right)}-\frac{k_yk_zv_{t-}^2\omega_{c}-}{\Omega_-^2\left(\omega_{c-}^2-\Omega_-^2\right)}\frac{\partial v_{0z-}}{\partial x}\right)}, \quad (5)$$

where $v_{t+}[=(\frac{T_+}{m_+})^{1/2}]$ and $v_{t-}[=(\frac{T_-}{m_-})^{1/2}]$ are the thermal velocities of positive and negative ions, $\omega_{c+}(=eB_s/m_+c)$ and $\omega_{c-}(=eB_s/m_-c)$ are the positive and negative ions cyclotron frequencies and $\Omega_+[=\omega-k_yv_{0y+}-k_zv_{0z+}]$ and $\Omega_-[=\omega-k_yv_{0y-}-k_zv_{0z-}]$ are the Doppler shifted wave frequencies for positive and negative ions, respectively.

Following the analysis of Sharma and Srivastava [19], the ion beam density perturbation is given by

$$n_{1b} = \frac{n_{0b}e(k_y^2+k_z^2)\phi_1}{m_b(\omega-k_zv_{0b})^2}, \quad (6)$$

where $k_y=k_\perp$ and $(k_y^2+k_z^2)\approx k^2(=k_\perp^2+k_z^2)$.

2.1. Infinite Boundary Effects

Using Eqs. (3)–(6) in the Poisson equation, $\nabla^2\phi_1=4\pi(n_{1e}e-n_{1+}e-n_{1b}e+n_{1-}e)$, we obtain,

$$1-\frac{\omega_{p+}^2v_{te}^2}{\omega_{pe}^2}\frac{\left(k_z^2-\frac{k_y^2\Omega_+^2}{\left(\omega_{c+}^2-\Omega_+^2\right)}+\frac{\lambda k_y\omega_{c+}\Omega_+}{\left(\omega_{c+}^2-\Omega_+^2\right)}-\frac{k_yk_z\omega_{c+}}{\left(\omega_{c+}^2-\Omega_+^2\right)}\frac{\partial v_{0z+}}{\partial x}\right)}{\left(\Omega_+^2-k_z^2v_{t+}^2+\frac{k_y^2v_{t+}^2\Omega_+^2}{\left(\omega_{c+}^2-\Omega_+^2\right)}-\frac{\lambda k_yv_{t+}^2\omega_{c+}\Omega_+}{\left(\omega_{c+}^2-\Omega_+^2\right)}+\frac{k_yk_zv_{t+}^2\omega_{c+}}{\left(\omega_{c+}^2-\Omega_+^2\right)}\frac{\partial v_{0z+}}{\partial x}\right)}$$
$$-\frac{\omega_{p-}^2v_{te}^2}{\omega_{pe}^2}\frac{\left(k_z^2-\frac{k_y^2\Omega_-^2}{\left(\omega_{c-}^2-\Omega_-^2\right)}-\frac{\lambda k_y\omega_{c-}\Omega_-}{\left(\omega_{c-}^2-\Omega_-^2\right)}+\frac{k_yk_z\omega_{c-}}{\left(\omega_{c-}^2-\Omega_-^2\right)}\frac{\partial v_{0z-}}{\partial x}\right)}{\left(\Omega_-^2-k_z^2v_{t-}^2+\frac{k_y^2v_{t-}^2\Omega_-^2}{\left(\omega_{c-}^2-\Omega_-^2\right)}+\frac{\lambda k_yv_{t-}^2\omega_{c-}\Omega_-}{\left(\omega_{c-}^2-\Omega_-^2\right)}-\frac{k_yk_zv_{t-}^2\omega_{c-}}{\left(\omega_{c-}^2-\Omega_-^2\right)}\frac{\partial v_{0z-}}{\partial x}\right)}=\frac{\omega_{pb}^2(k_y^2+k_z^2)v_{te}^2}{\omega_{pe}^2\left(\omega-k_zv_{0b}\right)^2} \quad (7)$$

where $\omega_{p+}[=(4\pi n_{0+}e^2/m_+)^{1/2}]$, $\omega_{p-}[=(4\pi n_{0+}e^2/m_-)^{1/2}]$, $\omega_{pb}[=(4\pi n_{0b}e^2/m_b)^{1/2}]$, $\omega_{pe}[=(4\pi n_{0e}e^2/m_e)^{1/2}]$ and $v_{te}[=(\frac{T_e}{m_e})^{1/2}]$ are the positive ion plasma frequency, negative ion plasma frequency, beam plasma frequency, electron plasma frequency and electron thermal velocity, respectively.

Equation (7) can be simplified further as

$$1-\frac{c_+^2}{(1-\varepsilon)}\frac{A^2}{\left(\Omega_+^2-v_{t+}^2A^2\right)}-\frac{\varepsilon c_-^2}{(1-\varepsilon)}\frac{B^2}{\left(\Omega_-^2-v_{t-}^2B^2\right)}=\frac{\omega_{pb}^2(k_y^2+k_z^2)v_{te}^2}{\omega_{pe}^2\left(\omega-k_zv_{0b}\right)^2}, \quad (8)$$

where $c_+(=T_e/m_+)^{1/2}$, $c_-(=T_e/m_-)^{1/2}$ are the positive ion and negative ion sound speeds, respectively,

$$A^2 = \left(k_z^2-\frac{k_y^2\Omega_+^2}{\left(\omega_{c+}^2-\Omega_+^2\right)}+\frac{\lambda k_y\omega_{c+}\Omega_+}{\left(\omega_{c+}^2-\Omega_+^2\right)}-\frac{k_yk_z\omega_{c+}}{\left(\omega_{c+}^2-\Omega_+^2\right)}\frac{\partial v_{0z+}}{\partial x}\right). \quad (9)$$

$$\text{and } B^2 = \left(k_z^2-\frac{k_y^2\Omega_-^2}{\left(\omega_{c-}^2-\Omega_-^2\right)}-\frac{\lambda k_y\omega_{c-}\Omega_-}{\left(\omega_{c-}^2-\Omega_-^2\right)}+\frac{k_yk_z\omega_{c-}}{\left(\omega_{c-}^2-\Omega_-^2\right)}\frac{\partial v_{0z-}}{\partial x}\right). \quad (10)$$

Equation (8) can be rewritten as

$$\left(\Omega_+^2 - P_+^2A^2\right)\left(\Omega_-^2 - P_-^2B^2\right) - \alpha A^2B^2 = \frac{\omega_{pb}^2(k_y^2+k_z^2)k^2v_{te}^2}{\omega_{pe}^2\left(\omega - k_zv_{0b}\right)^2}\left(\Omega_+^2 - v_{t+}^2A^2\right)\left(\Omega_-^2 - v_{t-}^2B^2\right), \tag{11}$$

where $P_+^2 = v_{t+}^2 + \frac{c_+^2}{(1-\varepsilon)}$, $P_-^2 = v_{t-}^2 + \frac{\varepsilon c_-^2}{(1-\varepsilon)}$, and $\alpha = \frac{\varepsilon c_+^2 c_-^2}{(1-\varepsilon)^2}$.

Equation (11) is the dispersion relation of an ion beam driven KHI in a plasma having negative ions. In the absence of beam, i.e., $n_{0b} \to 0$ or$\omega_{pb} = 0$, Eq. (11) reduces to

$$\left(\Omega_+^2 - P_+^2A^2\right)\left(\Omega_-^2 - P_-^2B^2\right) - \alpha A^2B^2 = 0. \tag{12}$$

Equation (12) is the dispersion relation of D'Angelo and Song [13] (cf. Eq. (26)). To study the interaction of an ion beam with positive and negative ions, we evaluate Eq. (8) for two different modes (i.e., K^+ and SF_6^- ion modes).

2.1.1. Beam Plasma Interaction with Positive Ions (K^+)

In the limit $\omega \sim \omega_{c+}$ and positive ion Larmor radius is less than the perpendicular wavelength of the positive ion mode, Eq. (8) can be rewritten as

$$1 - \frac{c_+^2}{(1-\varepsilon)}\frac{A^2}{\left(\Omega_+^2 - v_{t+}^2A^2\right)} = \frac{\omega_{pb}^2(k_y^2+k_z^2)v_{te}^2}{\omega_{pe}^2\left(\omega - k_zv_{0b}\right)^2}. \tag{13}$$

Equation (13) can be further rewritten as

$$(\Omega_+^2 - P_+^2A^2) = \frac{\omega_{pb}^2(k_y^2+k_z^2)v_{te}^2}{\omega_{pe}^2(\omega - k_zv_{0b})^2}(\Omega_+^2 - v_{t+}^2A^2). \tag{14}$$

We are looking for solutions when the beam is in Cerenkov resonance with the positive ion KHI mode. In the limit of long perpendicular wavelength, i.e., $k_y^2\Omega_+^2 \ll \omega_{c+}^2$, also, for low frequency approximations, i.e., $\Omega_+^2 \ll \omega_{c+}^2$ and in the absence of beam, i.e., $n_{0b} \to 0$ or $\omega_{pb} = 0$. Hence Eq. (14) gives

$$\left(\Omega_+^2 - \frac{\lambda k_yP_+^2}{\omega_{c+}}\Omega_+ - k_z^2P_+^2 + \frac{k_yk_zP_+^2}{\omega_{c+}}\frac{\partial v_{0z+}}{\partial x}\right) = 0, \tag{15}$$

and $\omega \cong k_zv_{0b}$.

Equation (16) corresponds to the positive ion KHI mode and $\omega \approx k_zv_{0b}$ corresponds to the beam mode. Let us write $\Omega_+ = \Omega_{r+} + i\Omega_{i+}$ and assume that wave is either weakly damped or growing (i.e., $|\Omega_{i+}| \ll \Omega_{r+}$). In the presence of beam, Eq. (15) can be simplified as

$$\zeta_+^2 - \frac{\Lambda_1\beta_1}{r}\zeta_+ - \frac{\gamma_1}{r}(\gamma_1 - \beta_1S_1) = 0, \tag{16}$$

where $\zeta_+ = \frac{\Omega_+}{\omega_{c+}}$ (here, $\zeta_+ = \zeta_{r+} + i\Gamma_+$), $\Lambda_1 = \lambda\rho_1$, $\beta_1 = k_y\rho_1$, $\gamma_1 = k_z\rho_1$, $S_1 = \frac{1}{\omega_{c+}}\frac{\partial v_{0z+}}{\partial x}$, $\rho_1^2 = \frac{\rho_+^2}{\omega_{c+}^2}$ (here, $\rho_+^2 = \mathrm{P}_+^2 - \frac{\omega_{pb}^2(k_y^2+k_z^2)v_{t+}^2v_{te}^2}{\omega_{pe}^2(\omega-k_zv_{0b})^2}$) and $r = (1 - \frac{\omega_{pb}^2(k_y^2+k_z^2)v_{te}}{\omega_{pe}^2(\omega-k_zv_{0b})^2})$.

Hence Eq. (16) gives the dispersion relation of Ion beam driven KHI for normalized positive ion mode. In the absence of beam (i.e., $\omega_{pb} \to 0, r = 1$), we can recover the dispersion relation of D'Angelo & Song [12] (cf. Eq. (23)) in the limit $\varepsilon \to Z\varepsilon$. For $T_e \simeq T_i$, we can recover the dispersion relation of D'Angelo [9] (cf. Eq. (15)). From Eq. (16) the maximized normalized growth rate $\Gamma_+(= \Omega_{i+}/\omega_{c+})$ can be found as

$$\Gamma_+ = \left[\frac{1}{4}\beta_1^2\left(\frac{S_1^2}{r} - \frac{\Lambda_1^2}{r^2}\right)\right]^{1/2}. \tag{17}$$

In the absence of beam and for $\varepsilon \to Z\varepsilon$, Eq. (17) is similar to the growth rate of Luo et al. [15] (cf. Eq. (2)).

2.1.2. Beam Plasma Interaction with Negative Ions (SF_6^-)

In the limit $\omega \sim \omega_{c-}$ and negative ion Larmor radius is less than the perpendicular wavelength of negative ion mode, Eq. (8) can be rewritten as

$$1 - \frac{\varepsilon c_-^2}{(1-\varepsilon)} \frac{B^2}{\left(\Omega_-^2 - v_{t-}^2 B^2\right)} = \frac{\omega_{pb}^2 (k_y^2 + k_z^2) v_{te}^2}{\omega_{pe}^2 \left(\omega - k_z v_{0b}\right)^2}. \tag{18}$$

Equation (18) can be further rewritten as

$$\left(\Omega_-^2 - P_-^2 B^2\right) = \frac{\omega_{pb}^2 \left(k_y^2 + k_z^2\right) v_{te}^2}{\omega_{pe}^2 \left(\omega - k_z v_{0b}\right)^2} \left(\Omega_-^2 - v_{t-}^2 B^2\right). \tag{19}$$

Again, we are looking for solutions when the beam is in Cerenkov resonance with the negative ion KHI mode. In the absence of beam, i.e., $\omega_{pb} = 0$ as $n_{0b} \to 0$, following the same procedure as was done earlier for positive ion mode, in the limit of long perpendicular wavelength, i.e., $k_y^2 \Omega_-^2 \ll \omega_{c-}^2$ and for low frequency approximations, i.e., $\Omega_-^2 \ll \omega_{c-}^2$, Eq. (19) gives

$$\left(\Omega_-^2 + \frac{\lambda k_y P_-^2}{\omega_{c-}} \Omega_- - k_z^2 P_-^2 - \frac{k_y k_z P_-^2}{\omega_{c-}} \frac{\partial v_{0z-}}{\partial x}\right) = 0, \tag{20}$$

and $\omega \cong k_z v_{0b}$.

Equation (20) corresponds to the negative ion KHI mode and $\omega \approx k_z v_{0b}$ corresponds to the beam mode. Let $\Omega_- = \Omega_{r-} + i\Omega_{i-}$. Assuming that the wave is either weakly damped or growing (i.e., $|\Omega_{i-}| \ll \Omega_{r-}$). Then in the presence of beam, Eq. (20) can be simplified in the same manner as was done for positive ion KHI mode as

$$\zeta_-^2 + \frac{\Lambda_2 \beta_2}{r} \zeta_- - \frac{\gamma_2}{r} (\gamma_2 + \beta_2 S_2) = 0, \tag{21}$$

where $\zeta_- = \frac{\Omega_-}{\omega_{c-}}$(here, $\zeta_- = \zeta_{r-} + i\Gamma_-$), $\Lambda_2 = \lambda \rho_2$, $\beta_2 = k_y \rho_2$, $\gamma_2 = k_z \rho_2$, $S_2 = \frac{1}{\omega_{c-}} \frac{\partial v_{0z-}}{\partial x}$, $\rho_2^2 = \frac{\rho_-^2}{\omega_{c-}^2}$ (here, $\rho_-^2 = \mathrm{P}_-^2 + \frac{\omega_{pb}^2 k^2 v_{t-}^2 v_{te}^2}{\omega_{pe}^2 (\omega - k_z v_{0b})^2}$), and $r = (1 - \frac{\omega_{pb}^2 k^2 v_{te}^2}{\omega_{pe}^2 (\omega - k_z v_{0b})^2})$.

Equation (21) gives the dispersion relation of ion beam driven KHI for normalized negative ion mode. From Eq. (21), the maximized normalized growth rate $\Gamma_-(= \Omega_{i-}/\omega_{c-})$ can be found as

$$\Gamma_- = \left[\frac{1}{4} \beta_2^2 \left(\frac{S_2^2}{r} - \frac{\Lambda_2^2}{r^2}\right)\right]^{1/2}. \tag{22}$$

In the absence of beam and for $\varepsilon \to Z\varepsilon$, Eq. (22) reduces to the growth rate expression of Luo et al. [15] (cf. Eq. (2)).

2.2. Finite Boundary Effects

Consider a plasma cylinder of radius a_1 consisting of electrons, positive ions K^+ (Potassium ions) and negative ions SF_6^- (Sulphur hexafluoride ions) immersed in the magnetic field B_s acting along positive z-direction and equilibrium densities of components $j(= e, +, -)$ vary along negative x-direction as $n_{0j} = \overline{n_{0j}} e^{-\lambda x}$ as for infinite boundaries. An ion beam with velocity $v_{0b} \parallel \hat{z}$, mass m_b, density $n_{0b} \ll n_{0+}$, and radius r_b propagates through plasma cylinder along the magnetic field. The other parameters are same as infinite geometry of plasma waveguide. Poisson equation can be simplified as a second order differential equation in ϕ_1, which can be rewritten for axially symmetric case as

$$\frac{\partial^2 \phi_1}{\partial r^2} + \frac{1}{r} \frac{\partial \phi_1}{\partial r} + p^2 \phi_1 = -\frac{\omega_{pb}^2 k^2 \phi_1}{(\omega - k_z v_{b0})^2}, \tag{23}$$

$$\text{where } p^2 = -k_z^2 - \frac{\omega_{pe}^2}{v_{te}^2} \left[1 - \frac{c_+^2}{(1-\varepsilon)} \frac{A_1^2}{\left(\Omega_+^2 - v_{t+}^2 A_1^2\right)} - \frac{\varepsilon c_-^2}{(1-\varepsilon)} \frac{B_1^2}{\left(\Omega_-^2 - v_{t-}^2 B_1^2\right)}\right] \tag{24}$$

$$\text{Also, } A_1^2 = \left(k_z^2 - \frac{k_\perp^2\,\Omega_+^2}{\left(\omega_{c+}^2 - \Omega_+^2\right)} + \frac{\lambda k_\perp \omega_{c+}\Omega_+}{\left(\omega_{c+}^2 - \Omega_+^2\right)} - \frac{k_\perp k_z \omega_{c+}}{\omega_{c+}^2 - \Omega_+^2}\frac{\partial v_{oz+}}{\partial x}\right) \tag{25}$$

$$\text{and } B_1^2 = \left(k_z^2 - \frac{k_\perp^2\,\Omega_-^2}{\left(\omega_{c-}^2 - \Omega_-^2\right)} - \frac{\lambda k_\perp \omega_{c-}\Omega_-}{\left(\omega_{c-}^2 - \Omega_-^2\right)} + \frac{k_\perp k_z \omega_{c-}}{\omega_{c-}^2 - \Omega_-^2}\frac{\partial v_{oz-}}{\partial x}\right). \tag{26}$$

In the absence of beam, i.e., $\omega_{pb} = 0$ as $n_{0b} \to 0$, the solution of Bessel equation Eq. (23) is given by

$$\phi_1 = AJ_0(p_m r), \tag{27}$$

where A is a constant, and the functions $J_o(p_m r)$ is called the zeroth-order Bessel functions of the first kind. At $r = a_1$, ϕ_1 must vanish, hence, $J_o(p_m a_1) = 0$, i.e., $p_m = \frac{x_n}{a_1}\,(n = 1, 2, \ldots), x_n$, are the zeros of the Bessel function $J_o(x)$.

If $J_o(x) = 0$ then $x = 2.404$ hence, $p_m = \frac{2.404}{a_1}$.

In the presence of the beam, the solution wave function ϕ_1 can be expressed in a series of orthogonal sets of wave functions:

$$\phi_1 = \sum\nolimits_m A_m J_o(p_n r). \tag{28}$$

Now substituting the value of Eq. (28) in Eq. (23), multiplying both sides of Eq. (23) by $rJ_o(p_n r)$ and integrating over r from 0 to a_1 (where a_1 is the plasma radius), retaining the dominant mode ($m = n$) only, we get

$$p^2 - p_m^2 = -\frac{\omega_{pb}^2 k^2 I}{(\omega - k_z\, v_{bo})^2}, \tag{29}$$

where $I = \frac{\int_0^{r_b} rJ_o(p_m r)J_o(p_n r)dr}{\int_0^{a_1} rJ_o(p_m r)J_o(p_n r)dr}$ and $k^2 = p_m^2 + k_z^2$.

Using the value of p^2 in Eq. (29) and simplifying, we obtain

$$1 - \frac{c_+^2}{(1-\varepsilon)}\frac{A_1^2}{\left(\Omega_+^2 - v_{t+}^2 A_1^2\right)} - \frac{\varepsilon c_-^2}{(1-\varepsilon)}\frac{B_1^2}{\left(\Omega_-^2 - v_{t-}^2 B_1^2\right)} = \frac{\omega_{pb}^2\left(p_m^2 + k_z^2\right)v_{te}^2 I}{\omega_{pe}^2\left(\omega - k_z v_{0b}\right)^2}. \tag{30}$$

Equation (30) is same as Eq. (8) of Infinite boundary analysis. On further simplifying Eq. (30), we get the similar dispersion relation as Eq. (11)

$$\left(\Omega_+^2 - P_+^2 A_1^2\right)\left(\Omega_-^2 - P_-^2 B_1^2\right) - \alpha A_1^2 B_1^2 = \frac{\omega_{pb}^2\left(p_m^2 + k_z^2\right)v_{te}^2 I}{\omega_{pe}^2\left(\omega - k_z v_{0b}\right)^2}\left(\Omega_+^2 - v_{t+}^2 A_1^2\right)\left(\Omega_-^2 - v_{t-}^2 B_1^2\right), \tag{31}$$

where $P_+^2 = v_{t+}^2 + \frac{c_+^2}{(1-\varepsilon)}$, and $P_-^2 = v_{t-}^2 + \frac{\varepsilon c_-^2}{(1-\varepsilon)}$, now we study the two modes of KHI for finite boundary effects in the same way as was done for infinite geometry effects.

2.2.1. Beam Plasma Interaction with Positive Ions (K^+)

In the limit $\omega \sim \omega_{c+}$ and positive ion Larmor radius is less than the perpendicular wavelength of the positive ion mode, Eq. (30) can be rewritten as

$$1 - \frac{c_+^2}{(1-\varepsilon)}\frac{A_1^2}{\left(\Omega_+^2 - v_{t+}^2 A_1^2\right)} = \frac{\omega_{pb}^2\left(p_m^2 + k_z^2\right)v_{te}^2 I}{\omega_{pe}^2\left(\omega - k_z v_{0b}\right)^2}. \tag{32}$$

Equation (32) can be further simplified in the absence of beam, i.e., $n_{0b} \to 0$ or $\omega_{pb} = 0$, in the limit of long perpendicular wavelength, i.e., $k_y^2\Omega_+^2 \ll \omega_{c+}^2$ and also, for low frequency approximations, i.e.,$\Omega_+^2 \ll \omega_{c+}^2$, to obtain the solutions when the beam is in Cerenkov resonance with the positive ion KHI mode. Hence Eq. (32) gives

$$\left(\Omega_+^2 - \frac{\lambda p_m P_+^2}{\omega_{c+}}\Omega_+ - k_z^2 P_+^2 + \frac{p_m k_z P_+^2}{\omega_{c+}}\frac{\partial v_{0z+}}{\partial x}\right) = 0, \tag{33}$$

and $\omega \cong k_z v_{0b}$.

Equation (33) corresponds to the positive ion KHI mode and $\omega \approx k_z v_{0b}$ corresponds to the beam mode. Following the same procedure as for infinite boundary, in the presence of beam, Eq. (32) can be further simplified as

$$\zeta_+^2 - \frac{\Lambda_1'\beta_1'}{r_1}\zeta_+ - \frac{\gamma_1'}{r_1}\left(\gamma_1' - \beta_1' S_1\right) = 0, \tag{34}$$

where $\zeta_+ = \frac{\Omega_+}{\omega_{c+}}(\zeta_+ = \zeta_{r+} + i\Gamma_+)$, $\Lambda_1' = \lambda\rho_1'$, $\beta_1' = p_m\rho_1'$, $\gamma_1' = k_z\rho_1'$, $S_1 = \frac{1}{\omega_{c+}}\frac{\partial v_{0z+}}{\partial x}$, $\rho_1'^2 = \frac{\rho_+'^2}{\omega_{c+}^2}$ (here, $\rho_+'^2 = P_+^2 - \frac{\omega_{pb}^2(p_m^2+k_z^2)v_{t+}^2 v_{te}^2 I}{\omega_{pe}^2(\omega - k_z v_{0b})^2}$) and $r_1 = (1 - \frac{\omega_{pb}^2(p_m^2+k_z^2)v_{te}^2 I}{\omega_{pe}^2(\omega - k_z v_{0b})^2})$.

Hence Eq. (34) gives the dispersion relation of ion beam driven KHI for normalized positive ion mode. From Eq. (34) the maximized normalized growth rate $\Gamma_+(= \Omega_{i+}/\omega_{c+})$ can be found as

$$\Gamma_+ = \left[\frac{1}{4}\beta_1'^2\left(\frac{S_1^2}{r_1} - \frac{\Lambda_1'^2}{r_1^2}\right)\right]^{1/2}. \tag{35}$$

2.2.2. Beam Plasma Interaction with Negative Ions (SF_6^-)

In the limit $\omega \sim \omega_{c-}$ and negative ion Larmor radius is less than the perpendicular wavelength of negative ion mode, Eq. (30) can be rewritten as

$$1 - \frac{\varepsilon c_-^2}{(1-\varepsilon)}\frac{B_1^2}{\left(\Omega_-^2 - v_{t-}^2 B_1^2\right)} = \frac{\omega_{pb}^2\left(p_m^2 + k_z^2\right)v_{te}^2 I}{\omega_{pe}^2\left(\omega - k_z v_{0b}\right)^2}. \tag{36}$$

Equation (36) can be further simplified to obtain solutions when the beam is in Cerenkov resonance with the negative ion KHI mode. In the limit of long perpendicular wavelength, i.e., $k_y^2\Omega_-^2 \ll \omega_{c-}^2$ and for low frequency approximations, i.e., $\Omega_-^2 \ll \omega_{c-}^2$, and in the absence of beam, i.e., $\omega_{pb} = 0$ as $n_{0b} \to 0$, Eq. (36) gives

$$\left(\Omega_-^2 + \frac{\lambda p_m P_-^2}{\omega_{c-}}\Omega_- - k_z^2 P_-^2 - \frac{p_m k_z P_-^2}{\omega_{c-}}\frac{\partial v_{0z-}}{\partial x}\right) = 0, \tag{37}$$

and $\omega \cong k_z v_{0b}$.

Equation (37) corresponds to the negative ion KHI mode and $\omega \approx k_z v_{0b}$ corresponds to the beam mode. Again following the same procedure as for infinite geometry, in the presence of beam, Eq. (37) can be simplified as

$$\zeta_-^2 + \frac{\Lambda_2'\beta_2'}{r_1}\zeta_- - \frac{\gamma_2'}{r_1}\left(\gamma_2' + \beta_2' S_2\right) = 0, \tag{38}$$

where $\zeta_- = \frac{\Omega_-}{\omega_{c-}}(\zeta_- = \zeta_{r-} + i\Gamma_-)$, $\Lambda_2' = \lambda\rho_2'$, $\beta_2' = p_m\rho_2'$, $\gamma_2' = k_z\rho_2'$, $\frac{1}{\omega_{c-}}\frac{\partial v_{0z-}}{\partial x} = S_2$, $r_1 = (1 - \frac{\omega_{pb}^2(p_m^2+k_z^2)v_{te}^2 I}{\omega_{pe}^2(\omega - k_z v_{0b})^2})$ and $\rho_2'^2 = \frac{\rho_-'^2}{\omega_{c-}^2}$, (here, $\rho_-'^2 = P_-^2 + \frac{\omega_{pb}^2(p_m^2+k_z^2)v_{t-}^2 v_{te}^2 I}{\omega_{pe}^2(\omega - k_z v_{0b})^2}$). Hence Eq. (38) gives the dispersion relation of an ion beam driven KHI for normalized negative ion mode. From Eq. (38), the maximized normalized growth rate $\Gamma_-(= \Omega_{i-}/\omega_{c-})$ can be found as

$$\Gamma_- = \left[\frac{1}{4}\beta_2'^2\left(\frac{S_2^2}{r_1} - \frac{\Lambda_2'^2}{r_1^2}\right)\right]^{1/2}. \tag{39}$$

The dispersion relations and the growth rate expressions obtained for finite boundaries of plasma waveguide are same as for infinite boundaries under certain limit.

3. RESULTS AND DISCUSSION

In the calculations, we have used plasma parameters for the experiments of An et al. [14] with some modification for infinite and finite boundary analysis of KHI modes. Using Eqs. (15) & (33) for the positive ions (K^+), we plot in Figs. 1(a) & 1(b) the dispersion curves of KHI with positive ion plasma for infinite and finite boundaries of plasma waveguide, respectively and using Eqs. (20) & (37) for negative ions (SF_6^-), the dispersion curves of KHI with negative ion plasma are plotted in Figs. 2(a) & 2(b), for infinite and finite boundaries of plasma waveguide, respectively, for the following parameters: plasma density $n_p = 1.0 \times 10^{11}\,\mathrm{cm}^{-3}$, positive ion density $n_{0+} = n_p$, relative

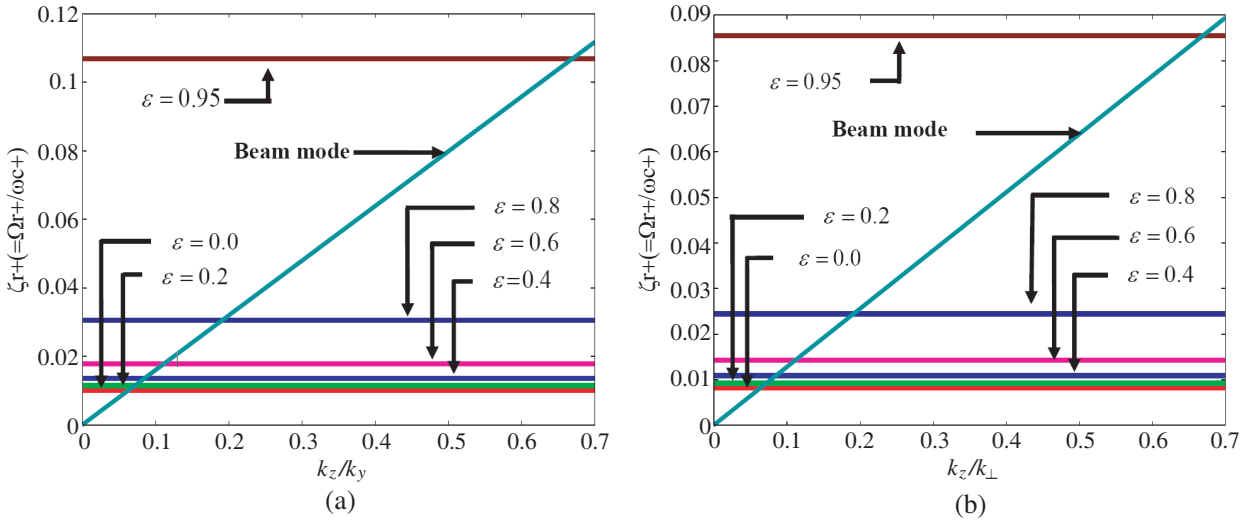

Figure 1. Dispersion curve between normalized real frequency of positive ion $\zeta_{r+}(= \Omega_{r+}/\omega_{c+})$ of the KHI for different values of the relative density of negative ions ε as a function of normalized wave vector k_z/k_y for (a) infinite and $k_z/k_\perp$, for (b) finite plasma boundary. The parameters are given in the text.

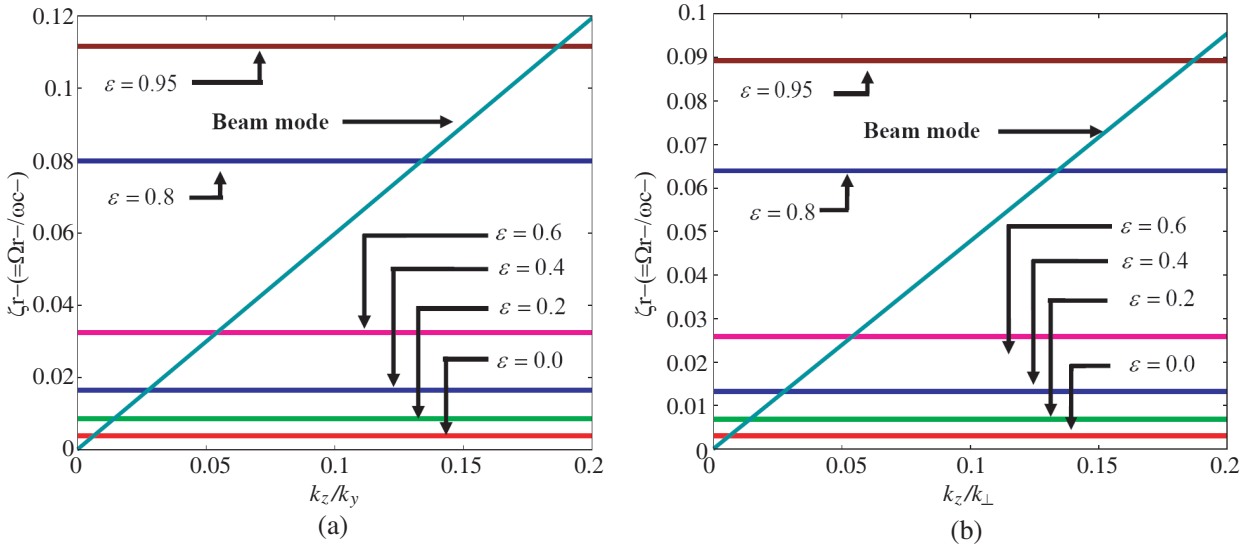

Figure 2. Dispersion curve between normalized real frequency of negative ion $\zeta_{r-}(= \Omega_{r-}/\omega_{c-})$ of the KHI for different values of relative density of negative ions ε as a function of normalized wave vector k_z/k_y for (a) infinite and $k_z/k_\perp$, for (b) finite plasma boundary. The parameters are same as Fig. 1.

Table 1. From Fig. 1 (ion beam + plasma with positive ions) we obtain the unstable wave frequencies Ω_{r+} (rad/sec) from normalized wave frequencies $\zeta_{r+}(=\Omega_{r+}/\omega_{c+})$, normalized wave vector k_z/k_y, axial wave vectors $k_z\,(\mathrm{cm}^{-1})$ and wavelength $\lambda_z\,(\mathrm{cm})$ for different values of ε & for infinite geometry case $k_y = 1.0\,\mathrm{cm}^{-1}$.

ε	k_z/k_y	$k_z\,(\mathrm{cm}^{-1})$	$\lambda_z\,(\mathrm{cm})$	Ω_{r+}/ω_{c+}	$\Omega_{r+}\,(\mathrm{rad/sec})$
0.0	0.063378	0.063378	99.09	0.010078	9.897×10^3
0.2	0.071544	0.071544	87.86	0.010357	10.171×10^3
0.4	0.084618	0.084618	74.22	0.013432	13.190×10^3
0.6	0.111554	0.111554	56.30	0.017895	17.572×10^3
0.8	0.190716	0.190716	32.93	0.030739	30.186×10^3
0.95	0.667368	0.667368	9.41	0.106673	104.753×10^3

Table 2. From Fig. 2 (ion beam + plasma with positive ions) we obtain the unstable wave frequencies Ω_{r+} (rad/sec) from normalized wave frequencies $\zeta_{r+}(=\Omega_{r+}/\omega_{c+})$, normalized wave vector $k_z/k_\perp$, axial wave vectors $k_z\,(\mathrm{cm}^{-1})$ and wavelength $\lambda_z\,(\mathrm{cm})$ for different values of ε for finite geometry case, where $k_\perp = p_m = 2.404/a_1 = 0.8\,\mathrm{cm}^{-1}$.

ε	$k_z/k_\perp$	$k_z\,(\mathrm{cm}^{-1})$	$\lambda_z\,(\mathrm{cm})$	Ω_{r+}/ω_{c+}	$\Omega_{r+}\,(\mathrm{rad/sec})$
0.0	0.064201	0.051361	122.38	0.008395	8.244×10^3
0.2	0.070755	0.056604	110.95	0.009237	9.071×10^3
0.4	0.083794	0.067035	93.77	0.010911	10.715×10^3
0.6	0.112377	0.089902	69.92	0.014472	14.212×10^3
0.8	0.190716	0.152573	41.16	0.024518	24.077×10^3
0.95	0.669015	0.535212	11.74	0.085240	83.706×10^3

density of negative ions $\varepsilon(=n_{SF_6^-}/n_{K^+}) = 0.0, 0.2, 0.4, 0.6, 0.8, 0.95$, electron temperature $T_e \simeq \mathrm{K}^+$ ion temperature $T_+ = 0.2\,\mathrm{eV}$, SF_6^- ion temperature $T_- = 0.2T_e$, plasma radius $a_1 = 3\,\mathrm{cm}$, beam radius $r_b = 2.5\,\mathrm{cm}$, guide magnetic field $B_s \simeq 4 \times 10^3\,\mathrm{Gauss}$ and $k_y \approx 1.0\,\mathrm{cm}^{-1}$, $k_z \approx 0 - 0.7\,\mathrm{cm}^{-1}$ and $\lambda \approx 2\,\mathrm{cm}^{-1}$. For finite geometry of plasma waveguide, k_y is given by the solution of Bessel function as $k_\perp = p_m = \frac{2.404}{a_1} = 0.84\,\mathrm{cm}^{-1}$, where a_1 = radius of cylindrical plasma waveguide. Real part of wave frequencies for positive and negative ion modes $\zeta_{r+}(=\Omega_{r+}/\omega_{c+})$ and $\zeta_{r-}(=\Omega_{r-}/\omega_{c-})$ have been plotted as a function of normalized wave vector k_z/k_y (for infinite geometry) & $k_z/k_\perp$ (for finite geometry) for different values of relative density of negative ions (cf. Figs. 1(a), 1(b), 2(a) & 2(b)) for both the positive and negative ion modes, respectively for infinite and finite geometry of waveguide. We have also plotted the beam mode for potassium ion beam energy $E_b = 0.5\,\mathrm{eV}$ or $v_{0b}[=(\frac{2E_b}{m_b})^{1/2}] = 1.567 \times 10^5\,\mathrm{cm/s}$. The frequencies and the corresponding wave numbers of the unstable waves are obtained by the point of intersections between the beam mode and positive ion KHI mode, for infinite and finite geometry of plasma waveguide and are given in Tables 1 & 2 and that for negative ion plasma KHI mode for infinite and finite geometry of plasma waveguide are given in Tables 3 & 4.

From Tables 1–4, we can say that the unstable wave frequencies of the KHI for positive as well as negative ion mode increase with the relative density of negative ions in the presence of beam. The frequency of positive ions increases by a factor ~ 0.33 when ε changes from 0.0 to 0.4 and increases by a factor ~ 1.28 when ε varies from 0.4 to 0.8 and by a factor ~ 2.47 with increase of ε from 0.8 to 0.95 for infinite geometry of plasma while for finite geometry of waveguide the frequency of positive ions increases by a factor ~ 0.30 when ε changes from 0.0 to 0.4 and increases by a factor ~ 1.25 when ε varies from 0.4 to 0.8 and by a factor ~ 2.47 with increase of ε from 0.8 to 0.95. The frequency of negative ions is found to increase by a factor ~ 3.26 when ε changes from 0.0 to 0.4 and increases by a factor ~ 3.76 when ε varies from 0.4 to 0.8 and by a factor ~ 0.39 with increase of ε from 0.8 to 0.95 for infinite boundaries and for finite boundaries the frequency of negative ions is found to increase by a

Table 3. From Fig. 3 (ion beam + plasma with negative ions) we obtain the unstable wave frequencies Ω_{r-} (rad/sec) from normalized wave frequencies $\zeta_{r-}(=\Omega_{r-}/\omega_{c-})$, normalized wave vector k_z/k_y, axial wave vectors $k_z\,(\mathrm{cm}^{-1})$ and wavelength $\lambda_z\,(\mathrm{cm})$ for different values of ε for infinite geometry case $k_y = 1.0\,\mathrm{cm}^{-1}$.

ε	k_z/k_y	$k_z\,(\mathrm{cm}^{-1})$	$\lambda_z\,(\mathrm{cm})$	Ω_{r-}/ω_{c-}	Ω_{r-} (rad/sec)
0.0	0.006216	0.006216	1011.23	0.003935	1.039×10^3
0.2	0.014382	0.014382	437.04	0.008683	2.292×10^3
0.4	0.027902	0.027902	225.07	0.016779	4.430×10^3
0.6	0.054029	0.054029	116.34	0.032412	8.557×10^3
0.8	0.133775	0.133775	46.94	0.079877	21.088×10^3
0.95	0.187176	0.187176	33.55	0.111142	29.342×10^3

Table 4. From Fig. 4 (ion beam + plasma with negative ions) we obtain the unstable wave frequencies Ω_{r-} (rad/sec) from normalized wave frequencies $\zeta_{r-}(=\Omega_{r-}/\omega_{c-})$, normalized wave vector $k_z/k_\perp$, axial wave vectors $k_z\,(\mathrm{cm}^{-1})$ and wavelength $\lambda_z\,(\mathrm{cm})$ for different values of ε for finite geometry case, $k_\perp = p_m = 0.8\,\mathrm{cm}^{-1}$.

ε	$k_z/k_\perp$	$k_z\,(\mathrm{cm}^{-1})$	$\lambda_z\,(\mathrm{cm})$	Ω_{r-}/ω_{c-}	Ω_{r-} (rad/sec)
0.0	0.006451	0.005161	1216.82	0.003279	0.866×10^3
0.2	0.014618	0.011694	537.03	0.007004	1.849×10^3
0.4	0.027441	0.021953	286.33	0.013285	3.507×10^3
0.6	0.054255	0.043404	144.82	0.026080	6.885×10^3
0.8	0.133775	0.107020	58.68	0.064001	16.896×10^3
0.95	0.187176	0.149741	41.94	0.089359	23.591×10^3

factor ~ 3.05 when ε changes from 0.0 to 0.4 and increases by a factor ~ 3.82 when ε varies from 0.4 to 0.8 and by a factor ~ 0.40 with increase of ε from 0.8 to 0.95. It can also be seen from the Tables 1–4 that the axial wave vector k_z increases with increasing ε. This result is similar to the analytical result of Chow and Rosenberg [28], where the wave is unstable because k_z increases with the relative density of negatively charged dust grains $\delta(=\frac{1}{1-Z\varepsilon})$.

We plot Fig. 3(a) using Eqs. (16) & (34), for normalized real frequency of KHI for positive ions and Fig. 3(b) using Eqs. (21) & (38), for normalized real frequency of KHI for negative ions as a function of relative density of negative ions ε in the absence and presence of beam for the same parameters as used for plotting Fig. 1 and Fig. 2, respectively, for infinite and finite geometry of plasma waveguide. It is observed that the unstable modes frequencies increase with the relative density of negative ions for both positive ion and negative ion modes under both infinite and finite boundaries of plasma waveguide. It is also observed that the KHI unstable modes frequencies slightly increase in the presence of beam at high concentration of negative ions. This result is in line with the experimental results obtained for electrostatic Ion Cyclotron waves (EICW) [29] (cf. Fig. 3, page No. 1555) and Ion Acoustic waves (IAW) [21] (cf. Fig. 1, page No. 285) in plasma with negative ions where the frequency of EICW and phase velocity of IAW increases with relative concentration of negative ions. For finite boundaries of plasma waveguide, the frequencies of KHI modes are lesser than for infinite boundary effects. These results are in line with the results for finite geometry effects obtained by Prakash et al. [27].

Using Eqs. (17) & (35), we plot Fig. 4(a), the normalized growth rate $\Gamma_+(=\Omega_{i+}/\omega_{c+})$ for positive ion mode of KHI, and using Eqs. (22) & (39), we plot Fig. 4(b), the normalized growth rate $\Gamma_-(=\Omega_{i-}/\omega_{c-})$ for negative ion KHI mode showing infinite and finite boundary effects, as a function of relative density of negative ions $\varepsilon(=0.0-1.0)$, respectively in the absence as well as in the presence of beam for the same parameters used for plotting Fig. 3 and for beam density $n_{b0} = 2.5 \times 10^8\,\mathrm{cm}^{-3}$ and the shear parameters $S_1 \simeq S_2(=0.7)$. It is observed that at a constant $\varepsilon = 0.7$ the growth rate of KHI for positive

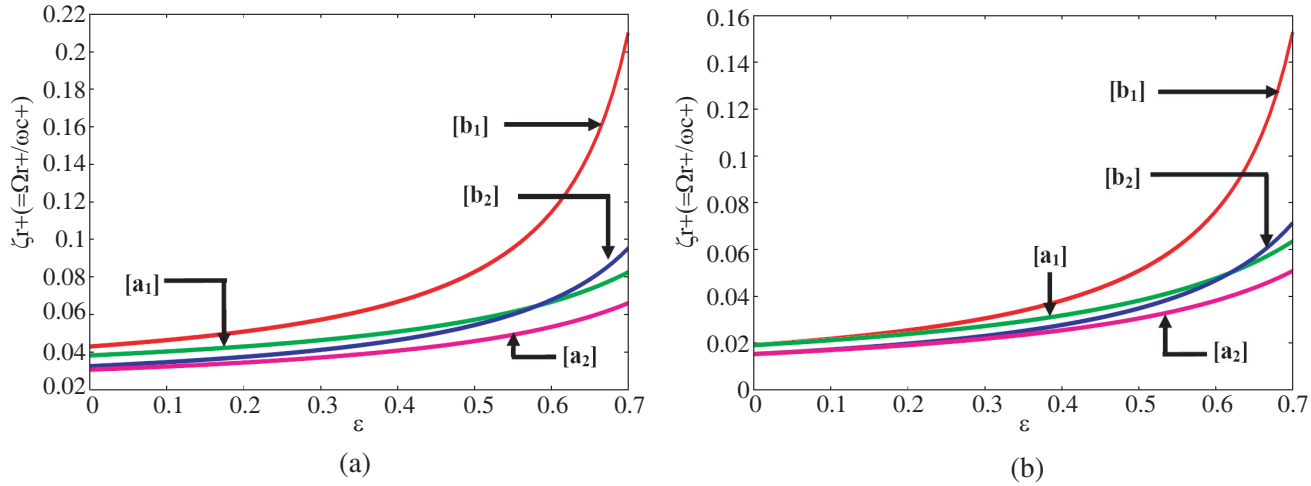

Figure 3. Normalized real frequency $\zeta_{rj}(=\Omega_{rj}/\omega_{cj})$ of the KHI (where $j(=+$ or $-)$, for positive ion and negative ion, respectively) for negative ions as a function of relative density of negative ions ε for infinite plasma boundary [a1] — in the absence of beam [b1] — in the presence of beam, and for finite plasma boundary, [a2] — in the absence of beam and [b2] — in the presence of beam for the parameters same as Fig. 2. (a) For Positive ion, (b) for Negative ion.

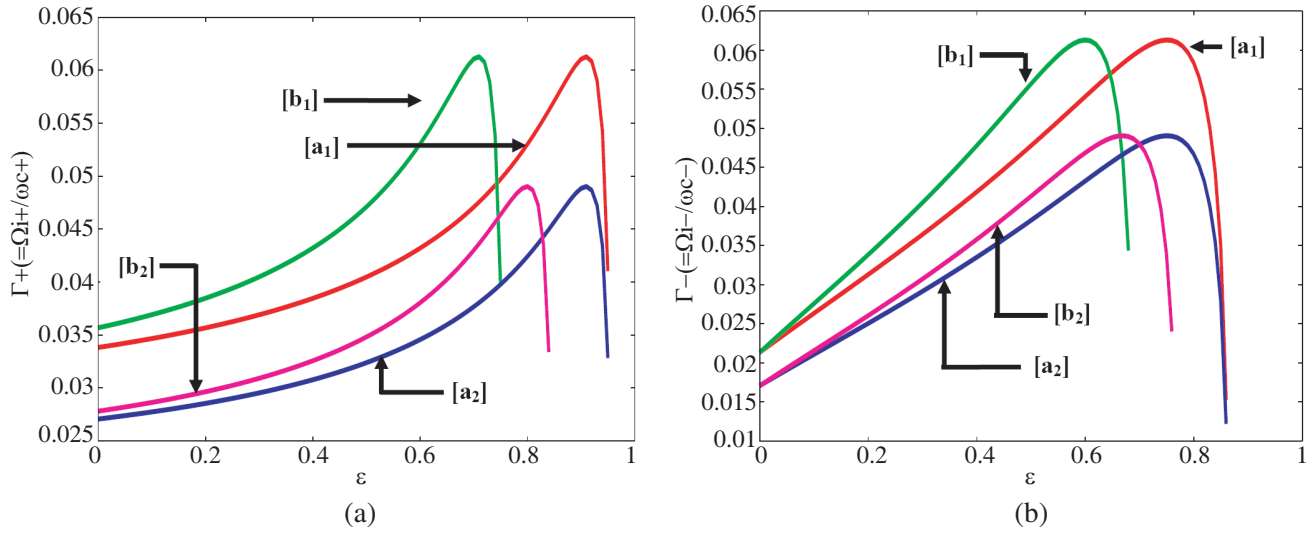

Figure 4. Normalized growth rate $\Gamma_j(=\Omega_{ij}/\omega_{cj})$ of the KHI (where $j(=+$ or $-)$, for positive and negative ions, respectively) as a function of the relative density of negative ions ε for infinite plasma boundary [a1] — in the absence of beam, [b1] — in the presence of beam, and for finite plasma boundary [a2] — in the absence of beam and [b2] — in the presence of beam for the same parameters as Fig. 3 and for beam density $n_{b0} = 2.5 \times 10^8\,\mathrm{cm}^{-3}$. (a) For Positive ions, (b) for Negative ions.

ions shoots up to 30% when the ion beam is switched on for infinite geometry of plasma waveguide. On the other hand for cylindrical waveguide, the growth rate of KHI positive ion mode increases only up to 14% in the presence of beam. For negative ions, at $\varepsilon = 0.6$ the growth rate of KHI increases up to 13% for infinite geometry in presence of beam while for finite geometry case increases only up to 8% in the presence of beam. From Figs. 4 (a) & (b), we can say that the growth rate of the KHI for both positive and negative ion modes increases with relative concentration of negative ions in the presence of beam for infinite as well as for finite geometry. Moreover, our results show the stabilizing effect of KHI for large concentration of negative ions. The results are in line with the experimental observations

of An et al. [14] (cf. Figs. 4 & 5 on page No. 50). It is also observed that the effect of beam on the destabilization of the KHI is prominent at large shear parameter and for large value of ε. This result is in line with the theoretical predictions of D'Angelo and Song [13] (cf. Figs. 1–5 on page No. 44–45), i.e., the growth rate of KHI is larger for large concentration of negative ions and for large shear parameters.

We also plot in Figs. 5 & 6 the normalized growth rate of KHI for the positive and negative ions, respectively, in presence of beam as a function of relative density of negative ions ε for different relative masses of negative ions (m_-/m_+) using the same parameters as that used for plotting Fig. 4, for infinite and finite geometries. From Figs. 5 & 6, it is observed that the KHI mode is stabilized for both the ion modes with increasing the relative mass of negative ions for infinite geometry of waveguide. These results are similar to the theoretical results of D'Angelo and Song [13] (cf. Fig. 6 on page No. 45). It is observed that the finite geometry effects further lowers the growth rate of positive ion while for negative ion growth rate of KHI shows an increase with relative mass of negative ions up to small values of ε and then decreases for large values of ε.

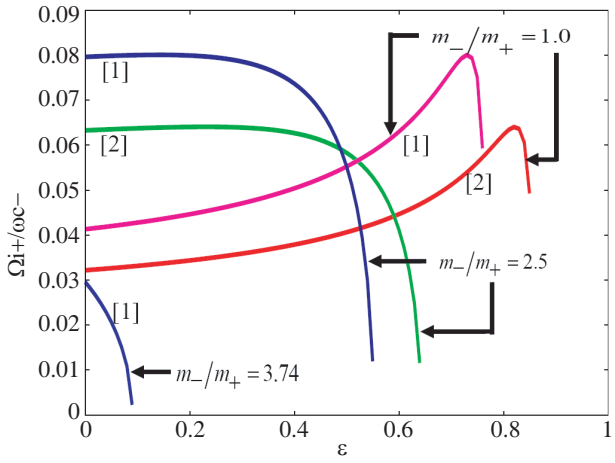

Figure 5. Normalized growth rate Ω_{i+}/ω_{c-} of the ion beam driven KHI for positive ions as a function of the relative density of negative ions ε for different relative masses of negative ions $m_-/m_+(= 1.0, 2.5, 3.74)$, [1] — for infinite boundary and [2] — for finite boundary of plasma waveguide. The parameters are same as Fig. 4.

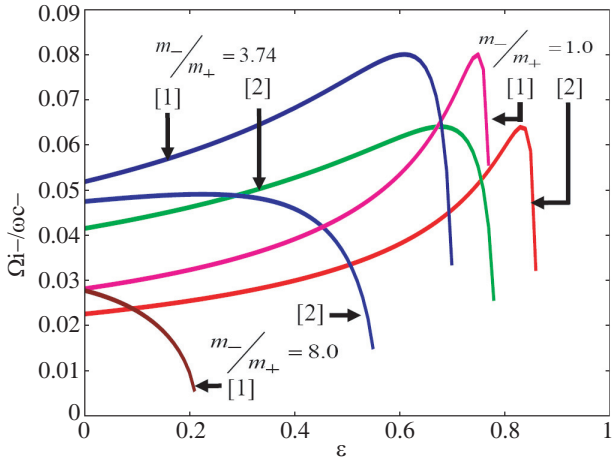

Figure 6. Normalized growth rate Ω_{i-}/ω_{c-} of the ion beam driven KHI for negative ions as a function of the relative density of negative ions ε for different relative masses of negative ions $m_-/m_+(= 1.0, 3.74, 8.0)$, [1] — for infinite boundary and [2] — for finite boundary of plasma waveguide for the same parameters as Fig. 4.

To investigate the effect of ion beam energies and densities on the growth rate of KHI in the presence of negative ions in the plasma, we plot the growth rate of KHI for both positive and negative ion modes as a function of relative density of negative ions in Figs. 7(a) & (b), respectively, for different values of beam velocities $v_{0b}[= (2E_b/m_b)^{1/2}] = 1.57 \times 10^5$, 3.57×10^5 and 7.0×10^5 cm/s, and Figs. 8(a) & (b), respectively, for different values of beam densities $n_{0b}(= 2.5 \times 10^7,\ 2.5 \times 10^8,\ 7.5 \times 10^8)\,\mathrm{cm}^{-3}$. Other parameters are the same as Fig. 4. It is found that the growth rate of KHI decreases at high beam energies or velocities while an increase of ion beam density boosts the growth rate of KHI modes.

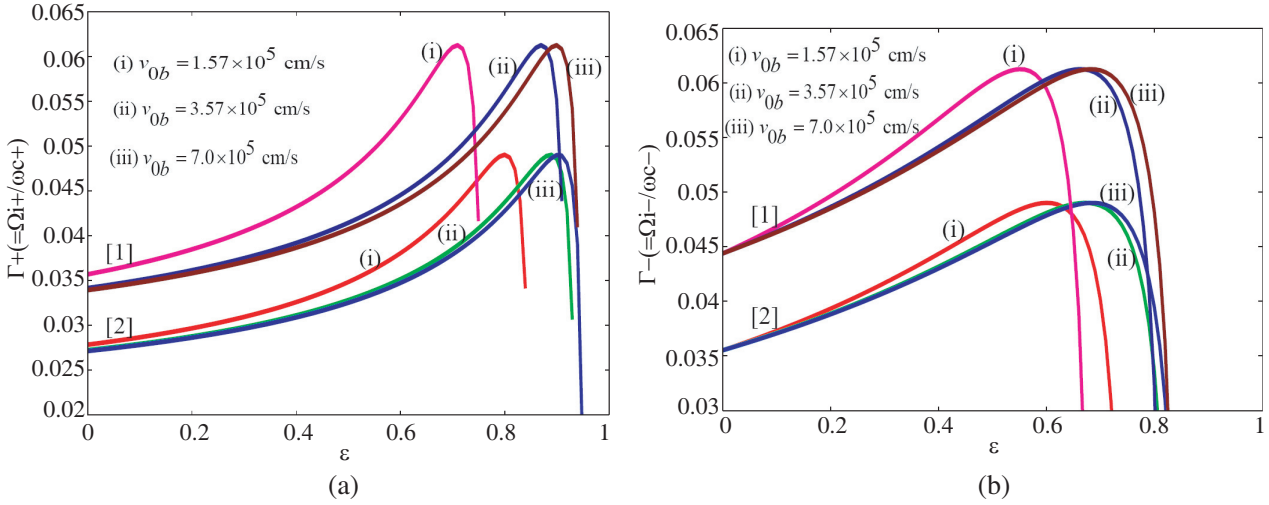

Figure 7. Normalized growth rate $\Gamma_j(= \Omega_{ij}/\omega_{cj})$ of the ion beam driven KHI (where $j(= +$ or $-)$, for positive and negative ions, respectively) as a function of the relative density of negative ions ε for different ion beam velocities $v_{0b}(= 1.57 \times 10^5, 3.57 \times 10^5, 7.0 \times 10^5)\,\mathrm{cm/s}$, [1] — for infinite boundary and [2] — for finite boundary of plasma waveguide, for the same parameters as Fig. 4, for (a) Positive ions, (b) Negative ions.

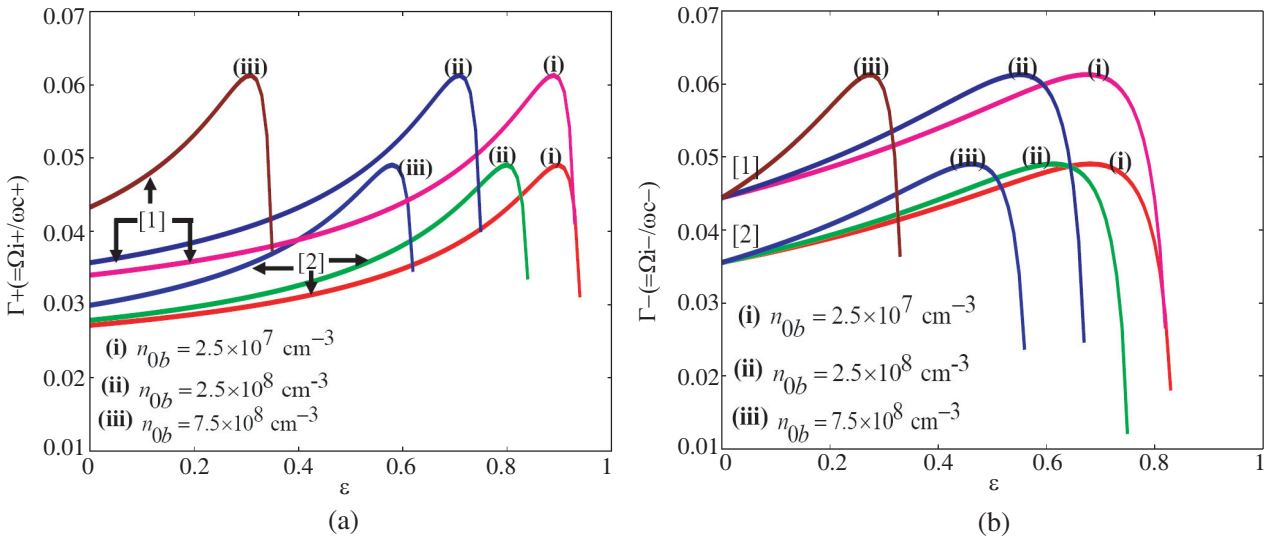

Figure 8. Normalized growth rate $\Gamma_j(= \Omega_{ij}/\omega_{cj})$ of the ion beam driven KHI (where $j(= +$ or $-)$, for positive and negative ions, respectively) as a function of the relative density of negative ions ε for different ion beam densities, $n_{0b}(= 2.5 \times 10^7, 2.5 \times 10^8, 7.5 \times 10^8)\,\mathrm{cm}^{-3}$, [1] — for infinite boundary and [2] — for finite boundary of plasma waveguide, for the same parameters as Fig. 7, for (a) Positive ions, (b) Negative ions.

4. CONCLUSIONS

The Kelvin Helmholtz instability (KHI) in a magnetized plasma having positive and negative ions is driven by an ion beam via a Cerenkov interaction.

The effect of beam on the growth of KHI is more prominently seen at high concentration of ε Our results are in line with the theoretical predictions of D'Angelo and Song [13] (cf. Figs. 1–5). It is also observed that KHI mode in presence of negative ions is destabilized up to $\varepsilon \leq 0.7$ and beyond this limit it is stabilized. This result is in line with the experimental observations of An et al. [14] (cf. Figs. 4 & 5 on page No. 50). Our results show stabilization of KHI mode up to $\varepsilon \leq 0.6$ in the presence of negative ions and the ion beam. The results also show that the KHI mode is stabilized in presence of heavier negative ions in the potassium plasma which is similar to the result obtained by D'Angelo and Song [13] (cf. Fig. 6 on page No. 45). A comparison of finite and infinite geometry effects describe that the frequency and growth rate of KHI is reduced for cylindrical plasma waveguide, it may be due to reduction in beam plasma interaction region [27]. The results showing increase in frequency and growth rate of Low frequency KHI modes are in line with the experimental observations of electrostatic ion Cyclotron waves [29] and Ion Acoustic waves [21] in negative ion plasma. An increase in beam energy reduces the growth rate of KHI while increase of beam density enhances the growth rate of the KHI modes. Our theoretical model of KHI driven by an ion beam in negative ion plasma may be validated via laboratory and space plasma experiments in near future.

In addition, our results of KHI, in general, may be useful for understanding the instabilities in the negative ion plasma in the material processing [30–32] (as the velocity shear instability and negative ions in plasma plays an important role in surface technologies) beam plasma system [33] (as ion beam tends to excite the instabilities in plasma) various fluids phenomena [34] such as Magneto hydrodynamic flows and the properties of Earth's ionosphere [2–7, 35] such as solar wind, ion loss on Mars and energy transport in space etc. However, the results need to be verified for above applications via experiments/simulations for definite evidences as we have basically emphasized on the laboratory plasma.

REFERENCES

1. D'Angelo, N., "Ultralow frequency fluctuations at the polar cusp boundaries," *J. Geophys. Res.*, Vol. 78, No. 7, 1206–1209, 1973.
2. Pu, Z. Y. and M. G. Kivelson, "Kelvin Helmholtz instability at magnetopause: Energy flux into magnetosphere," *J. Geophys. Res.*, Vol. 88, No. A2, 853–861, 1983.
3. Miura, A., "Kelvin Helmholtz instability for supersonic shear flow at the magnetospheric boundary," *Geophys. Res. Lett.*, Vol. 17, No. 6, 749–752, 1990.
4. Hasegawa, H., M. Fujimoto, T. D. Phan, H. Réme, A. Balogh, M. W. Dunlop, C. Hashimoto, and R. T. Dokoro, "Transport of solar wind into Earth's magnetosphere through rolled-up Kelvin-Helmholtz vortices," *Nature*, Vol. 430, No. 7001, 755–758, 2004.
5. Migliuolo, S., "Velocity shear instabilities in the anisotropic solar wind and the heating of ions perpendicular to the magnetic field," *J. Geophys. Res.*, Vol. 89, No. A1, 27–36, 1984.
6. Ershkovich, A. I., "Kelvin-Helmholtz instability in type-1 comet tails and associated phenomena," *Space Sci. Rev.*, Vol. 25, No. 1, 3–34, 1980.
7. Penz, T., N. V. Erakaev, H. K. Biernet, H. Lammer, U. V. Amerstorfer, H. Gunell, E. Kallio, S. Barabash, S. Orsini, A. Milillo, and W. Baumjohann, "Ion loss Mars caused by Kelvin-Helmholtz instability," *Planet. Space Sci.*, Vol. 52, No. 13, 1157–1167, 2004.
8. Chandrasekhar, S., *Hydrodynamic and Hydromagnetic Stability*, Chap. XI, 481, Clarendon Press, Oxford, 1961.
9. D'Angelo, N., "Kelvin-Helmholtz instability in a fully ionized plasma in a magnetic field," *Phys. Fluids*, Vol. 8, No. 9, 1748–1750, 1965.
10. D'Angelo, N. and S. V. Goeler, "Investigation of Kelvin Helmholtz instability in a cesium plasma," *Phys. Fluids*, Vol. 9, No. 2, 309–313, 1966.
11. Smith, C. G. and S. V. Goeler, "The Kelvin-Helmholtz instability in a collisionless plasma model," *Phys. Fluids*, Vol. 11, No. 12, 2665–2668, 1968.

12. D'Angelo, N. and B. Song, "The Kelvin-Helmholtz instability in dusty plasmas," *Planet. Space Sci.*, Vol. 38, No. 12, 1577–1579, 1990.
13. D'Angelo, N. and B. Song, "Kelvin-Helmholtz instability in a plasma with negative ions," *IEEE Trans. Plasma Sci.*, Vol. 19, No. 1, 42–46, 1991.
14. An, T., R. L. Merlino, and N. D'Angelo, "The effect of negative ions on the Kelvin-Helmholtz instability in a magnetized potassium plasma," *Phys. Lett. A*, Vol. 14, No. 1–2, 47–52, 1996.
15. Luo, Q. Z., N. D'Angelo, and R. L. Merlino, "The Kelvin-Helmholtz instability in a plasma with negatively charged dust," *Phys. Plasmas*, Vol. 8, No. 1, 31–35, 2001.
16. Ostrikov, K., "Surface science of plasma exposed surfaces — A challenge for applied plasma science," *Vacuum*, Vol. 83, No. 1, 4–10, 2008.
17. Ostrikov, K., S. Kumar, and H. Sugai, "Charging and trapping of macroparticles in near-electrode regions of fluorocarbon plasmas with negative ions," *Phys. Plasmas*, Vol. 8, No. 7, 3490–3497, 2001.
18. Ostrikov, K., "Colloquium: Reactive plasmas as a versatile nano fabrication tool," *Rev. Mod. Phys.*, Vol. 77, No. 2, 489–511, 2005.
19. Sharma, S. C. and M. P. Srivastava, "Ion beam driven ion cyclotron waves in a plasma cylinder with negative ions," *Phys. Plasmas*, Vol. 8, No. 3, 679–686, 2001.
20. Sharma, S. C. and A. Gahlot, "Ion beam driven ion-acoustic waves in a plasma cylinder with negative ions," *Phys. Plasmas*, Vol. 15, No. 7, 0737051–0737056, 2008.
21. Song, B., N. D'Angelo, and R. L. Merlino, "Ion-acoustic waves in a plasma with negative ions," *Phys. Fluids B*, Vol. 3, No. 2, 284–287, 1991.
22. An, T., R. L. Merlino, and N. D' Angelo, "Lower hybrid waves in a plasma with negative ions," *Phys. Fluids B*, Vol. 5, No. 6, 1917–1918, 1993.
23. D'Angelo, N. and R. L. Merlino, "Electrostatic ion-cyclotron waves in a plasma with negative ions," *IEEE Trans. Plasma Sci.*, Vol. 14, No. 3, 285–286, 1986.
24. Rosenberg, M. and R. L. Merlino, "Ion-acoustic instability in a dusty negative ion plasma," *Planet. Space Sci.*, Vol. 55, No. 10, 1464–1469, 2007.
25. Yatsui, K. and Y. Yamamoto, "Heating of plasma ions by a modulated beam," *Phys. Letters*, Vol. 30A, No. 2, 135–136, 1969.
26. Chang, R. P., "Lower hybrid beam-plasma instability," *Phys. Rev. Lett.*, Vol. 35, No. 5, 285–288, 1975.
27. Prakash, V., S. C. Sharma, Vijayshri, and R. Gupta, "Ion beam driven resonant ion-cyclotron instability in a magnetized dusty plasma," *Phys. Plasmas*, Vol. 21, No. 3, 0337011–0337016, 2014.
28. Chow, V. W. and M. Rosenberg, "Electrostatic ion cyclotron instabilities in negative ion plasmas," *Plasma Phys.*, Vol. 3, No. 4, 1202–1211, 1996.
29. Kim, S. H., J. R. Heinrich, and R. L. Merlino, "Electrostatic ion-cyclotron waves in a plasma with heavy negative ions," *Planet. Space Sci.*, Vol. 56, No. 11, 1552–1559, 2008.
30. Tyagi, R. K., R. S. Pandey, and A. Kumar, "Surface coating by velocity shear instability in plasma," *Theoretical Foundations of Chem. Engg.*, Vol. 46, No. 5, 508–514, 2012.
31. Stoffels, E., W. W. Stoffels, and G. M. W. Kroesen, "Plasma chemistry and surface processes of negative ions," *Plasma Sources Sci. Technol.*, Vol. 10, No. 1, 311–317, 2001.
32. Kuznetsova, V. P., S. Yu. Tarasov, and A. I. Dmitriev, "Nanostructuring burnishing and subsurface shear instability," *Journ. of Mat. Processing Tech.*, Vol. 217, No. 1, 327–335, 2015.
33. Rosenberg, M. and P. K. Shukla, "Instability of ion flows in bounded dusty plasma systems," *Phys. Plasmas*, Vol. 5, No. 10, 3786, 1998.
34. Matsuoka, C., "Kelvin-Helmholtz instability and roll-up," *Scholarpedia*, Vol. 9, No. 3, 11821, 2014.
35. Moore, T. W., K. Nykyri, and A. P. Dimmock, "Cross-scale energy transport in space plasmas," *Nature Physics*, 2016, doi:10.1038/nphys3869.